Substitutional carbon in germanium

L. Hoffmann, J. C. Bach, and B. Bech Nielsen
Institute of Physics and Astronomy, Aarhus University, DK-8000, Aarhus C, Denmark

P. Leary and R. Jones
Department of Physics, University of Exeter, EX44QL, Exeter, United Kingdom

S. Öberg
Department of Mathematics, University of Luleå, S-95 187, Luleå, Sweden
(Received 27 November 1996)

Carbon impurities implanted into single-crystalline germanium are studied with infrared absorption spectroscopy and ion channeling. After implantation of $^{12}C^+$ at room temperature and subsequent annealing at 350 °C, a sharp infrared absorption line is observed at 531 cm^{-1}. When $^{12}C^+$ is substituted by $^{13}C^+$, the line shifts down in frequency to 512 cm^{-1} and co-implantation of $^{12}C^+$ and $^{13}C^+$ does not give rise to additional lines. Therefore, the 531-cm^{-1} line represents a local vibrational mode of a defect containing a single carbon atom. Channeling measurements are carried out around the ⟨100⟩, ⟨110⟩, and ⟨111⟩ axes in $^{12}C^+$-implanted samples annealed at 450 °C. The analysis of the data shows that 31 ± 3 % of the carbon atoms are located at substitutional sites, while the remaining carbon atoms appear to be located randomly. The population of the substitutional site and the intensity of the 531-cm^{-1} mode have identical temperature dependencies. It is concluded that the 531-cm^{-1} mode is the three-dimensional T_2 stretch mode of substitutional carbon. The effective charge of the mode is determined to be $(3.4\pm0.5)e$. *Ab initio* local density functional cluster theory is applied to calculate the structure and the local vibrational modes of substitutional carbon in germanium. The calculated frequencies and isotope shifts for the T_2 stretch mode are in good agreement with the observations. [S0163-1829(97)14317-X]

I. INTRODUCTION

Carbon is an important impurity in silicon, and its properties have been intensively studied for decades.[1] As a result of this, several carbon defects have been identified, of which the most prominent one is substitutional carbon.[2,3] This defect has tetrahedral (T_d) symmetry, with the carbon atom forming four equivalent covalent bonds with its silicon neighbors. The Si-C bonds are substantially shorter ($\sim$0.3 Å) (Refs. 4 and 5) than the normal Si-Si bonds, which results in a considerable strain field around the defect. Due to its high symmetry, substitutional carbon has a single three-dimensional local mode (T_2 mode) with a frequency of 607 cm^{-1} (see Ref. 2).

At first glance, substitutional carbon is expected to exist also in germanium, since silicon and germanium have similar chemical properties. The dissociation energy of the Ge-C bond is high,[6] $\sim$4.7 eV, compared to the $\sim$2.8 eV required to break a Ge-Ge bond. This supports the formation of substitutional carbon in germanium. However, the Ge-C bond length in molecular compounds[7] is $\sim$1.9 Å, much shorter than the 2.41 Å long Ge-Ge bond. This implies that the strain field around substitutional carbon in germanium will be very large. Therefore, the balance between the energy gained in forming Ge-C bonds and the increase in energy to accommodate the strain may make the formation of the substitutional carbon defect unfavorable. For example, the strain could be relieved by forming interstitial carbon or an interstitial-substitutional carbon defect, both of which have been observed in silicon.[8,9] The fact that the solubility of carbon in germanium is very low[10] (10^8–10^{10} cm^{-3}) compared to the solubility of carbon in silicon[11] (3.5×10^{17} cm^{-3}) indicates that strain may play an important role.

The present work addresses this problem, both experimentally and theoretically. With a combination of infrared absorption spectroscopy and ion channeling, a local mode of substitutional carbon in germanium is identified. The local vibrational mode frequency and the isotope shifts calculated by *ab initio* theory are in close agreement with those observed.

II. EXPERIMENTAL DETAILS

Samples with typical dimensions of $\sim10\times10\times0.5$ mm^3 were cut from high-resistivity float-zone-grown single-crystalline germanium with an oxygen content below 10^{16} cm^{-3}. The 10×10 mm^2 surfaces were perpendicular to either a ⟨100⟩, a ⟨110⟩, or a ⟨111⟩ crystal axis and both surfaces were mechanically polished.

The samples were implanted with $^{12}C^+$ and/or $^{13}C^+$ ions at 11 different energies ranging from 50 to 450 keV as specified in Table I. The dose implanted at each energy (see Table I) was adjusted to yield an almost uniform carbon concentration of 0.7 at. % (3×10^{20} cm^{-3}) from 0.1 to 0.8 μm below the surface of the sample, as shown in Fig. 1. One sample was co-implanted with $^{12}C^+$ and $^{13}C^+$ ions into overlapping profiles so that the local concentration of each isotope was 0.7 at. %. The implantations were carried out at room tem-

TABLE I. Energies (in keV) and doses (in 10^{15} cm^{-2}) used for implantation of $^{12}C^+$ and $^{13}C^+$.

Energy	50	75	100	125	150	200	250	300	350	400	450
^{12}C dose	1.30	1.09	1.96	0.44	2.17	2.17	2.17	2.17	2.17	2.17	2.17
^{13}C dose	1.33	1.11	1.56	0.44	2.22	2.22	2.22	2.22	2.22	2.22	2.22

perature with a background pressure of 2×10^{-6} torr. The normal of the 10×10 mm^2 surfaces was tilted 7° off the direction of the carbon beam to reduce channeling effects, and the beam was swept horizontally and vertically across the sample to ensure a homogeneous lateral distribution of implants. The sample was electrically insulated from the vacuum chamber, and the dose was determined directly from integration of the current to the sample. Emission of secondary electrons was suppressed with a shield surrounding the sample kept at -200 V relative to ground.

Most samples were annealed at 450 °C after the implantation since this leads to a maximum intensity of the infrared absorption line investigated in this work. The annealing was performed in a furnace with a continuous nitrogen-gas flow. The temperature was stable to within ±2 °C, and the annealing time was 20 min. Prior to the annealing and before each measurement, all samples were etched with 1% HF to remove surface oxides.

After the implantation and 450 °C anneal, all samples investigated by channeling were mechanically polished to remove surface carbon deposited during the implantation process. Approximately 0.1 μm of the sample was removed in this way. The associated loss of the implanted carbon was always less than 10%. After this the samples were annealed at 440 °C to remove the near-surface damage introduced by the polishing.

The infrared-absorption measurements were performed with a Nicolet System 800 Fourier-transform spectrometer, equipped with a closed-cycle helium cryocooler for optical measurements. The measurements were carried out in the spectral range from 400 to 7000 cm^{-1} using a Ge-KBr beam splitter, a globar light source, and a triglycine sulfate (TGS) or a mercury-cadmium-telluride (MCT) detector. The apodized resolution was 2 cm^{-1}, and the optical beam-spot was about 3 mm in diameter. A reference absorbance spectrum measured on a non implanted germanium crystal was subtracted from the sample absorbance spectra.

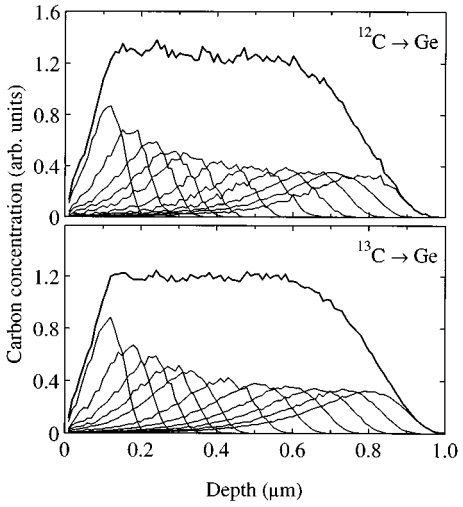

FIG. 1. TRIM simulations (Ref. 12) of the carbon profiles in germanium.

The channeling technique and the experimental setup have been described in detail previously,[13,14] and only a brief account will be given here. The sample was placed in a computer-controlled motor-driven x-y goniometer with an angular resolution of $\sim0.01°$. The goniometer was mounted in a vacuum chamber pumped to a pressure of $\sim3\times10^{-6}$ torr by a diffusion pump equipped with a liquid-nitrogen cryotrap. The sample was kept at room temperature during the measurements, but was surrounded by an electrically insulated cryoshield held at ~120 K to reduce carbon buildup on the surface during the experiment.

The channeling measurements were carried out with a 1300-keV deuteron beam supplied by a HVEC 5-MeV Van de Graaff accelerator. The beam was collimated by two 1×1 mm^2 slits 4 m apart, resulting in a beam divergence of $\sim0.01°$. The implanted ^{12}C atoms were probed by means of the nuclear reaction $^{12}C(d,p)^{13}C$ (see Ref. 15), detecting the 3.25-MeV protons in a large-area (4.9-cm^2) solid-state detector (the proton detector) located at $\sim135°$ relative to the beam direction and at a distance of 3.5 cm from the sample. In front of this detector, a 30-μm aluminum foil was placed to stop the deuterons backscattered from the germanium host and, thereby, avoid severe dead-time problems.

The backscattered deuterons were monitored simultaneously with another solid-state detector [the Rutherford backscattering (RBS) detector] also at an angle of $\sim135°$ relative to the beam direction and with a small acceptance angle. The yield of backscattered deuterons was integrated over a depth interval corresponding to the range of the implanted carbon profile.

The energy dependence of the proton yield of the $^{12}C(d,p)^{13}C$ nuclear reaction was measured directly using a 1500-Å graphite foil with a carbon density of 2.0 g cm^{-3} as target. On basis of this, the energy of the deuteron beam applied in the measurements was chosen to be 1300 keV. With this choice, the cross section of the nuclear reaction is within 4% constant over the carbon depth profile. The stopping powers of the incoming deuterons may differ about a factor of 2 between the channeled and nonchanneled particles. However, this difference corresponds only to $\sim2\%$ variation in the cross section integrated over the implanted region.

The angle between the crystal axis and the analyzing beam is conventionally denoted the *tilt angle*, and the yield measured at large tilt angles (a few degrees) is denoted the *random yield*. Irradiation on a fresh beamspot with 10 μC of the analyzing beam in the aligned direction (zero tilt angle) led to a decrease of less than 5% in the proton random yield. This decrease is associated with a beam-induced loss of car-

bon from the sample, most likely from the sample surface. Irradiation beyond 10 μC in a random or the aligned direction did not produce any further carbon loss. Therefore, prior to the channeling measurement, each spot on the sample was irradiated with 10-μC deuterons in the aligned direction.

With a fixed beam fluence, the yield of backscattered deuterons was measured simultaneously as a function of tilt angle. These angular distributions of yield, denoted yield curves, were measured for all major axes. The yield at each tilt angle was measured as an average over all azimuthal angles[14] to average out effects of planar channeling and to obtain a reliable random yield, which is used to normalize the data. The total fluence at each tilt angle was 2 μC, the beam spot size was $1\times1\ \mathrm{mm}^2$, and the beam current was 5–7 nA, measured on the target with the cryoshield biased to -500 V. In order to reduce the effects of radiation damage, the yield curves were always measured in a sequence going from the center of the axis towards larger tilt angles.

A virgin germanium crystal was mechanically polished and subsequently annealed at 440 °C as described above. Measurements on this sample showed no buildup of surface carbon during the channeling analysis. Moreover, proton-yield curves measured on this sample showed that the carbon is located on either the surface or randomly in the bulk.

Channeling and infrared absorption measurements were carried out on the same sample after 20-min anneals at several temperatures, starting at 450 °C (see Ref. 16) and moving up to 700 °C in steps of $\sim$50 °C. A fresh beam spot for the channeling measurement was chosen for each temperature, and the infrared absorbance spectrum was measured around the same spot. Within 10%, the channeling measurement did not produce any changes in the infrared-absorption signal.

III. RESULTS

After implantation of $^{12}C^+$ in germanium and subsequent annealing at 450 °C, a single sharp absorption line is observed at 531 cm^{-1} as can be seen in Fig. 2(a). This line shifts down to 512 cm^{-1} when ^{12}C is substituted by ^{13}C [see Fig. 2(b)]. The frequency ratio between the two lines is 1.037, which differs by only 0.4% from $\sqrt{13/12}$, i.e., the frequency ratio expected for a carbon atom bound by a harmonic potential to a rigid lattice.[17] Therefore, the 531-cm^{-1} line represents a local vibrational mode of carbon bound to X, where X is heavy and almost certainly germanium. The spectrum obtained after co-implantation of $^{12}C^+$ and $^{13}C^+$ with overlapping profiles is shown in Fig. 2(c). No new modes appear, and thus the 531-cm^{-1} mode originates from a defect containing a single carbon atom.

The angular distributions of proton and deuteron yields around the three major axes are shown in Fig. 3. For all three axes, there is a dip in the proton yield when the beam is aligned with the axis. The widths of the dips are close to those for backscattered deuterons, but the normalized minimum yields for the protons are much higher than those for the deuterons. Only a substitutional (perfect lattice site) or near-substitutional sites are consistent with broad dips in yield for all three major axes.[14,18] A significant fraction of the carbon atoms are consequently located at substitutional or near-substitutional sites. The solid lines through the data

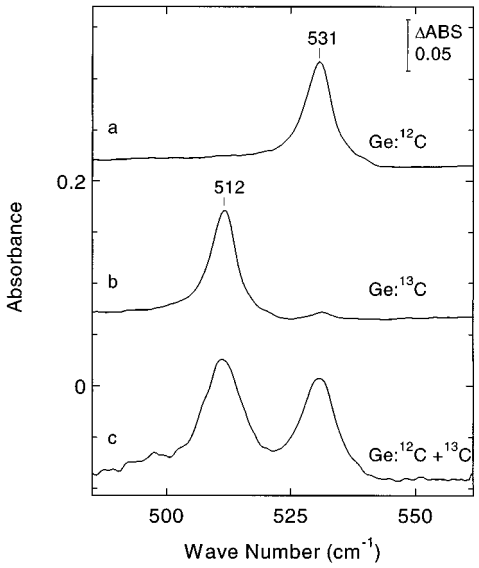

FIG. 2. Sections of absorbance spectra measured at 9 K on samples annealed at 450 °C after implantation with (a) $^{12}C^+$, (b) $^{13}C^+$, and (c) co-implantation with equal doses of both isotopes.

points in the figure represent the best fit to the data. This fit corresponds to 31 ± 3 % of the carbon atoms located at substitutional sites while the remaining 69 ∓ 3 % are located randomly.

In this analysis, the yield curves for substitutional carbon have been assumed equal to the host dips in yield of backscattered deuterons. This is of course an approximation since the vibrational amplitude for carbon differs from that of germanium. However, with the local vibrational mode identified above, the root-mean-square value of the one-dimensional vibrational amplitude of carbon is expected to be $\sim\sqrt{\hbar/m\omega}=0.073$ Å, which is close to the germanium value of 0.085 Å estimated from a Debye model.[19] Rather than using the experimental host dips in yield, it is possible to rely on computer simulations[14] of the curves for substitutional carbon. These simulations are based on a perfect lattice.

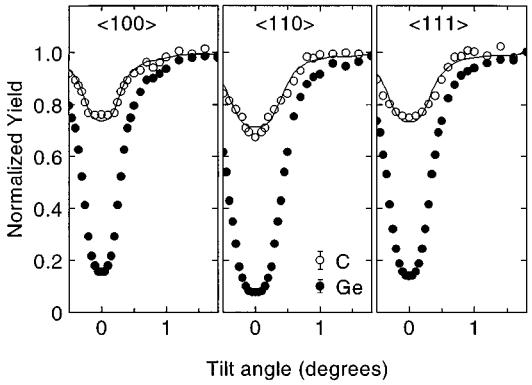

FIG. 3. Angular distributions of normalized yield measured around the ⟨100⟩, ⟨110⟩, and ⟨111⟩ axis after annealing at 450 °C. The best fit (solid line) to the carbon data (○) is obtained with (31 ± 3)% carbon at substitutional sites, while the remaining carbon atoms are randomly located. The fit is obtained using the host curve data (●) to approximate the curve for substitutional carbon. Typical statistical uncertainties are also indicated.

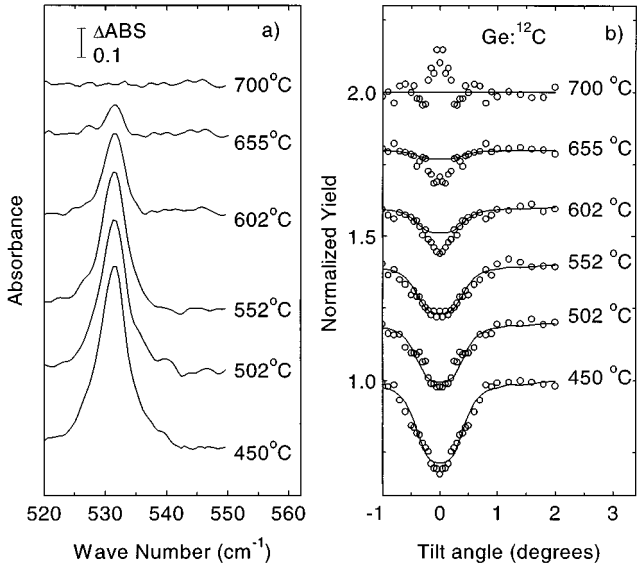

FIG. 4. Effects of annealing on (a) the absorbance spectrum and (b) the ⟨110⟩ proton-yield curve. Note that the different curves have been displaced vertically with respect to one another. The solid lines in part (b) of the figure represent the best fits at large tilt angles from which the population of the substitutional sites is determined.

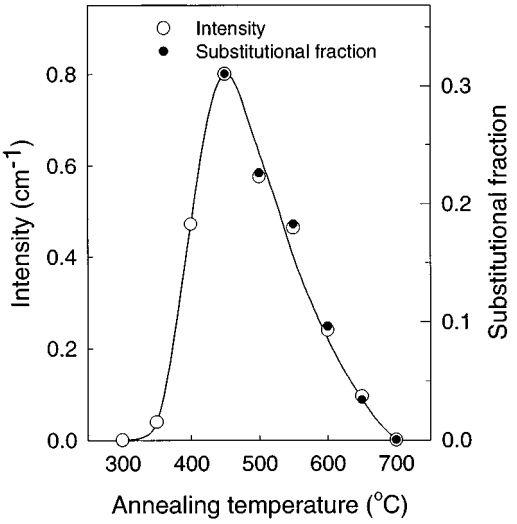

FIG. 5. Intensity of the 531-cm^{-1} line (○) and population of carbon atoms at substitutional sites (●) shown as a function of annealing temperature. The scales of the y axes are chosen so that the two sets of data overlap at 450 °C. The solid line is drawn to guide the eye.

Now, the experimental values of the host minimum yields for the ⟨100⟩, ⟨110⟩, and ⟨111⟩ axes are 0.16, 0.08, and 0.14, which are substantially higher than the respective values 0.09, 0.05, and 0.08 measured on a virgin crystal. Therefore, this approach has not been pursued.

The computer simulations have, however, been applied to estimate an upper limit on the displacement of the near-substitutional carbon from a substitutional site. The simulations are based on the continuum model[20] and include the effect of dechanneling from the perfect lattice.[14,21] Furthermore, the thermal vibrations of host and carbon atoms are included. The one-dimensional vibrational amplitude of the host is taken to be 0.085 Å, as mentioned above, and the same value is applied for the carbon atom. The yield curves corresponding to carbon atoms displaced from lattice sites along various directions have been simulated. It is found that the observed dips in proton yields originate from carbon atoms which at most are displaced 0.2 Å from lattice sites.

The effects of isochronal annealing in the temperature range from 450 to 700 °C on the 531-cm^{-1} mode and the ⟨110⟩ yield curves are shown in Fig. 4. The 531-cm^{-1} mode begins to appear at 350 °C and reaches maximum intensity at 450 °C. Annealing at higher temperatures leads to a decrease in the intensity, and eventually at 700 °C, the mode has disappeared.

The changes in the ⟨110⟩ proton-yield curves are slightly more complicated. At 450 °C, a broad dip is observed which is associated with the substitutional lattice site as discussed above. When the temperature is increased, the population of substitutional sites decreases, and at 602 °C, the dip starts to narrow, which shows that a new well-defined carbon structure is formed at this temperature. At 700 °C, the substitutional dip is completely gone and yet a new structure is formed which gives rise to a peak at zero tilt angle. Thus, at least qualitatively, the annealing of the 531-cm^{-1} mode occurs in parallel with the depopulation of the substitutional sites. A more quantitative analysis has been made to investigate this point further. At large tilt angles (0.6°–1°), only the substitutional site gives a normalized yield significantly different from the random value. Therefore, the population of the substitutional sites can be determined from a fit to this part of the proton-yield curves. The solid lines in Fig. 4(b) represent these fits. The result of the analysis is shown in Fig. 5 where the population of the substitutional sites is shown together with the intensity of the 531-cm^{-1} mode as a function of annealing temperature. The scales of the y axes are chosen so that the two sets of data overlap at 450 °C. It is evident from Fig. 5 that the annealing of the 531-cm^{-1} mode occurs parallel to the depopulation of the substitutional site.

IV. THEORETICAL CALCULATIONS

The structure and the local vibrational mode frequencies of substitutional carbon in germanium have been calculated using *ab initio* local density functional cluster theory.[22] The calculations were made on 71- and 131-atom tetrahedral clusters $Ge_{35}H_{36}$ and $Ge_{71}H_{60}$, where the central germanium atom was replaced by carbon and the dangling bonds on the surface of the cluster are terminated by hydrogen. Norm-conserving pseudopotentials were used for germanium and carbon.[23] The electronic wave functions and the charge density were fitted using s- and p-type Gaussian orbitals centered on the atomic nuclei and at the center of every Ge-C and Ge-Ge bond. We used eight Gaussian orbitals with different exponents on the carbon atom and four Gaussian orbitals on each of the inner 16 germanium atoms. A fixed linear combination of four Gaussian orbitals was used for the remaining germanium atoms. For the terminating hydrogen atoms another linear combination of three Gaussians was used. In addition to the atomic basis, three s- and p-type Gaussians were placed at the center of every bond. The self-consistent energy and forces on the atoms were calculated,

TABLE II. Calculated bond lengths (in Å) and local vibrational mode frequencies (in cm^{-1}) for substitutional carbon in germanium. The experimental local vibrational mode frequencies are included for comparison.

	Ge-C bond	Ge-Ge bond	^{12}C	^{13}C	^{14}C
Experiment			531	512	
71-atom cluster	2.018	2.415	563	542	524
131-atom cluster	1.046	2.447	516	497	480

and then every atom was moved via a conjugate gradient algorithm until the total energy was minimized. In the starting configuration the carbon and all germanium atoms were located at lattice sites for a pure germanium crystal. A full T_d symmetry constraint was imposed for the relaxations, leading to the energy minimum configuration. To calculate the local vibrational modes of the defect, the energy second derivatives with respect to atomic positions were calculated directly for the carbon atom and its four germanium neighbors, while a Musgrave-Pople potential[24,25] was used for the remaining germanium atoms. In this way, the full dynamical matrix of the cluster was constructed. The 71- and 131-atom clusters yielded almost identical structures, with the Ge-C bond lengths within 1.3% of each other. All the results are summarized in Table II, and below the results from the 131-atom cluster are discussed.

The energy minimization results in a configuration where substitutional carbon exerts a large tensile strain on the surrounding atoms (see Fig. 6). The Ge-C bond lengths are 2.046 Å, 18% shorter than the bulk Ge-Ge bond length of 2.407 Å. As a result of this, the Ge-Ge back bonds are increased in length by 1.6% to 2.447 Å. The highest vibrational mode frequency is 516 cm^{-1}, well above the Raman frequency at 304 cm^{-1}. This mode is triply degenerate (T_2) and involves the vibration of the carbon atom and, to a much lesser extent, its four neighbors. The frequency of the mode drops by 19 and 36 cm^{-1} when ^{12}C is substituted with ^{13}C and ^{14}C, respectively.

V. DISCUSSION

The experimental findings show that the 531-cm^{-1} mode originates from a defect containing a single carbon atom. Moreover, the correlation between the depopulation of the substitutional site and the loss of intensity of the 531-cm^{-1} mode establishes that the defect involves a single substitutional carbon. The concentrations of substitutional carbon in our samples are $\sim 10^{20}$ cm^{-3} and are thus orders of magnitude higher than that of any other impurity. Therefore, the involvement of other impurities can be disregarded. The same argument cannot be used to rule out the involvement of intrinsic defects in the structure. However, it is hard to imagine that a carbon atom interacting with a vacancy-type or interstitial-type defect would be located exactly at a substitutional site. Moreover, the symmetry of such a defect would be lower than tetrahedral in which case at least two carbon modes should be expected, but only one is observed. On this basis, we identify the 531-cm^{-1} mode as the triply degenerate T_2 mode of isolated substitutional carbon in germanium. This mode mainly involves vibration of the carbon atom and to a much lesser extent vibrations of the nearby germanium atoms.

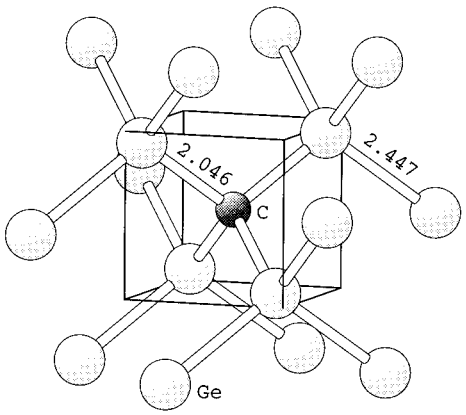

FIG. 6. Structure of substitutional carbon in germanium calculated from *ab initio* theory. The bond lengths are in Å.

Additional support to this identification comes from the vibrational frequency of substitutional carbon in silicon. Ratios of stretch mode frequencies in similar molecular compounds containing Si-C and Ge-C bonds are given in Table III. As can be seen from the table, the frequency ratio between Si-C and Ge-C modes varies between 1.068 and 1.165 with an average value of 1.132. With this ratio, the frequency for the vibrational mode of substitutional carbon in germanium is estimated to be 536 cm^{-1} from the frequency of 607 cm^{-1} for substitutional carbon in silicon. This value is very close to the 531 cm^{-1} actually observed.

The *ab initio* calculations provide further support for our identification. The calculated frequency of the local vibrational mode of substitutional carbon is found in the range of 516–563 cm^{-1}, well within the 100-cm^{-1} limit which is typical of the method. Furthermore, when ^{12}C is substituted with ^{13}C, the calculated mode drops by 19 cm^{-1}, which compares extremely well with the experimental reduction.

The effective (or apparent) charge η of a substitutional impurity of mass m_{imp} present in a concentration N is defined by[28,29]

TABLE III. Carbon-related vibrational frequencies ω (in cm^{-1}) of similar molecular compounds containing Si or Ge (Refs. 26 and 27). The ratio given is ω(Si-C)/ω(Ge-C). X denotes either Si or Ge.

Compound	ω(Si-C)	ω(Ge-C)	Ratio
CH_3XH_3	701	602	1.165
$X(CH_3)_4$	598	560	1.068
	696	599	1.162

$$\int \alpha(\omega)d\omega = \frac{2\pi^2\eta^2 N}{ncm_{\mathrm{imp}}}, \quad (1)$$

where α is the absorption coefficient associated with the local mode, $n=3.99$ is the refractive index, and c is the velocity of light. The number of carbon atoms at substitutional sites and, thereby, N can be determined directly from the channeling measurements using the proton yield from the carbon foil as a reference. The effective charge of the 531-cm^{-1} mode may now be determined from the intensity of the mode via Eq. (1). It is found that $\eta=(3.4\pm0.5)e$, where e is the elementary charge. Thus, the effective charge of substitutional carbon in germanium is comparable to the corresponding values in silicon[30,31] and GaAs,[32] which are $2.4e$ and $3.0e$, respectively. With the value of η established, it is possible to estimate or to give an upper limit on the concentration of substitutional carbon in germanium from infrared spectroscopy.

VI. CONCLUSION

The substitutional carbon defect in germanium has been identified by a combination of infrared absorption spectroscopy, ion channeling, and *ab initio* theory. The defect is observed after carbon implantation and subsequent annealing above 350 °C, and it possesses a local vibrational T_2 stretch mode at 531 cm^{-1}. The calculated frequency is in good agreement with this value, and the calculated isotope shift is in excellent agreement with our observations. The effective charge of the T_2 mode is found to be $\eta=(3.4\pm0.5)e$, which is comparable to the corresponding values in silicon and GaAs.

ACKNOWLEDGMENTS

This work has been supported by the Danish National Research Foundation through Aarhus Center for Advanced Physics (ACAP). P.L. and R.J. thank the HPCI for computer time on the T3D where some of this work was carried out. S.Ö. thanks NFR and TFR in Sweden for financial support and, also, PDC at KTH for computer time on the SP2.

[1] For a recent review, see G. Davies and R. C. Newman, in *Handbook on Semiconductors*, edited by T. S. Moss (Elsevier Science, Amsterdam, 1994), Vol. 3b, p. 1557, and references therein.

[2] R. C. Newman and J. B. Willis, J. Phys. Chem. Solids **26**, 373 (1965).

[3] J. W. Strane, S. R. Lee, H. J. Stein, S. T. Picraux, J. K. Watanabe, and J. W. Mayer, J. Appl. Phys. **79**, 637 (1996).

[4] G. G. DeLeo, W. B. Fowler, and G. D. Watkins, Phys. Rev. B **29**, 3193 (1984).

[5] R. Jones and S. Öberg, Semicond. Sci. Technol. **7**, 27 (1992).

[6] A. G. Gaydon, *Dissociation Energies and Spectra of Diatomic Molecules*, 3rd ed. (Chapman & Hall, London, 1968).

[7] *CRC Handbook of Chemistry and Physics*, 73rd ed., edited by D. R. Lide (CRC Press, Boca Raton, FL, 1993). The stated Ge-C bond length is that of the CH_3GeH_3 molecule.

[8] A. R. Bean and R. C. Newman, Solid State Commun. **8**, 175 (1970).

[9] L. W. Song, X. D. Zhan, B. W. Benson, and G. D. Watkins, Phys. Rev. B **42**, 5765 (1990).

[10] R. I. Scace and G. A. Slack, J. Chem. Phys. **30**, 1551 (1959).

[11] A. R. Bean and R. C. Newman, J. Phys. Chem. Solids **32**, 1211 (1971).

[12] J. F. Ziegler, J. P. Biersack, and U. Littmark, *The Stopping and Range of Ions in Solids* (Pergamon, New York, 1985).

[13] L. C. Feldman, J. W. Mayer, and S. T. Picraux, *Materials Analysis by Ion Channeling* (Academic, New York, 1982).

[14] B. Bech Nielsen, Phys. Rev. B **37**, 6353 (1988).

[15] During the implantation of $^{12}C^+$ ions, carbon was deposited on the sample surface. A way to circumvent this problem is to implant $^{13}C^+$ and use the $^{13}C(d,p)^{14}C$ nuclear reaction. However, the cross section for that reaction is about 40 times lower than that for the $^{12}C(d,p)^{13}C$ reaction, which implies that the crystal would be exposed to $\sim$40 times higher fluences during an axial scan. This would lead to extreme dechanneling, and therefore we apply the $^{12}C(d,p)^{13}C$ reaction.

[16] It has not been possible to carry out channeling measurements when the annealing temperature was below 450 °C due to insufficient recrystallization.

[17] In a real crystal the host atoms also vibrate. This is normally taken into account by assigning an effective mass μ_c to the carbon atom, given by $\mu_c^{-1}=m_c^{-1}+(\chi M)^{-1}$, where m_c is the mass of the carbon isotope, M is the mass of the host atom bonded to carbon, and χ is a factor which accounts for the geometry and the coupling to the lattice. χ is unknown, but it is of the order of unity. When $M \gg m_c$, the frequency ratio of the two carbon isotopes does not, therefore, differ substantially from $\sqrt{13/12}$.

[18] F. Berg Rasmussen and B. Bech Nielsen, Phys. Rev. B **49**, 16 353 (1994).

[19] D. S. Gemmel, Rev. Mod. Phys. **46**, 129 (1974).

[20] J. Lindhard, K. Dan. Vidensk. Selsk. Mat. Fys. Medd. **34**, 14 (1965).

[21] E. Bonderup, H. Espersen, J. U. Andersen, and H. E. Schiøtt, Radiat. Eff. **12**, 261 (1972).

[22] R. Jones, Philos. Trans. R. Soc. London, Ser. A **341**, 351 (1992).

[23] G. B. Bachelet, D. R. Hamann, and M. Schlüter, Phys. Rev. B **26**, 4199 (1982).

[24] M. J. P. Musgrave and J. A. Pople, Proc. R. Soc. London, Ser. A **268**, 474 (1962).

[25] F. Berg Rasmussen, R. Jones, and S. Öberg, Phys. Rev. B **50**, 4378 (1994).

[26] A. Clark and A. Weber, J. Chem. Phys. **45**, 1759 (1966).

[27] H. Siebert, Z. Anorg. Allg. Chem. **263**, 82 (1950).

[28] R. C. Newman, in *Imperfections in III/V Materials, Vol. 38 of Semiconductors and Semimetals*, edited by E. R. Weber (Academic, Boston, 1993), p. 117.

[29] It may be noted that η defined in Eq. (1) is merely an experimen-

tal parameter and not a true charge. If local field corrections are neglected, η^2/m_{imp} is equal to the square of the derivative of the dipole moment with respect to a normal coordinate of the mode.

[30] R. C. Newman and R. S. Smith, J. Phys. Chem. Solids **30**, 1493 (1969).

[31] S. P. Chappell, M. Claybourn, R. C. Newman, and K. G. Barraclough, Semicond. Sci. Technol. **3**, 1047 (1988).

[32] M. R. Brozel, E. J. Foulkes, R. W. Series, and D. T. J. Hurle, Appl. Phys. Lett. **49**, 339 (1986).